Anal. Chem. **2011,** *83,* 254–260

Surface-Enhanced Raman Scattering Detection of DNA Derived from the West Nile Virus Genome Using Magnetic Capture of Raman-Active Gold Nanoparticles

Hao Zhang, Mark H. Harpster, Hee Joon Park, and Patrick A. Johnson*

Department of Chemical and Petroleum Engineering, University of Wyoming, Laramie, Wyoming 82071, United States

William C. Wilson

Center for Grain and Animal Health Research, Arthropod Borne Animal Research Unit, Manhattan, Kansas 66502, United States

A model paramagnetic nanoparticle (MNP) assay is demonstrated for surface-enhanced Raman scattering (SERS) detection of DNA oligonucleotides derived from the West Nile virus (WNV) genome. Detection is based on the capture of WNV target sequences by hybridization with complementary oligonucleotide probes covalently linked to fabricated MNPs and Raman reporter tag-conjugated gold nanoparticles (GNPs) and the subsequent removal of GNP−WNV target sequence−MNP hybridization complexes from solution by an externally applied magnetic source. Laser excitation of the pelleted material provided a signature SERS spectrum which is diagnostic for the reporter, 5,5′-dithiobis(succinimidy-2-nitrobenzoate) (DSNB), and restricted to hybridization reactions containing WNV target sequences. Hybridizations containing dilutions of the target oligonucleotide were characterized by a reduction in the intensification of the spectral peaks accorded to the SERS signaling of DSNB, and the limit of detection for target sequence in buffer was 10 pM. Due to the short hybridization times required to conduct the assay and ease with which reproducible Raman spectra can be acquired, the assay is amenable to adaptation within a portable, user-friendly Raman detection platform for nucleic acids.

In recent years, surface-enhanced Raman scattering (SERS) spectroscopy has garnered considerable attention as a promising analytical tool for the development of novel biosensor assays. The potential biomedical applications of SERS-based assays have been demonstrated for tumor imaging and cancer therapeutics,[1−3] as well as a host of developed immunoassays and nucleic acid detection schemes, which are designed to be competitive with existing enzyme-linked immunosorbent assay (ELISA) and quantitative real-time polymerase chain reaction (qRT-PCR) diagnostic technologies.[4−6] Although diagnostic products based on SERS have yet to be commercialized, SERS affords an opportunity for adaptability to universal detection platforms that afford a number of advantages over fluorescence-based assays. These include the absence of photobleaching for Raman scattering compounds, or tags, the large number of Raman tags which can be selected for different experimental design applications, and the high information content provided by Raman tags upon laser excitation.[7] Due to the narrow spectrum peak widths characteristic of inelastic light scattering, SERS is uniquely suited for high-level multiplex detection and resolution.

Assays developed for the SERS-based detection of nucleic acids have largely focused on the capture of synthetic oligonucleotides using Au or Ag SERS-active nanoparticles (NP) and planar surface substrates fabricated with nonoverlapping complementary oligonucleotide probes. Upon hybridization, target sequences are detected by the localization of Raman reporter tags within laser elicited "hot spot" electromagnetic junctures determined by the spatial positioning of SERS substrate sandwich and aggregate complexes. Employing microarray detection formats in which oligonucleotide capture probes are organized as ordered arrays on solid-surface support chips, target sequence limit of detection (LOD) sensitivities ranging from 1 μM to 50 nM have been reported[8−10] and the four- to eight-plex detection of unrel-

* To whom correspondence should be addressed. E-mail: pjohns27@uwyo.edu. Fax: 307-766-6777.

(1) Kennedy, D. C.; Duguay, D. R.; Tay, L.-L.; Richeson, D. S.; Pezacki, J. P. *Chem. Commun.* **2009**, *44*, 6750–6752.
(2) Jun, B.-H.; Noh, M. S.; Kim, J.; Kim, G.; Kang, H.; Kim, M.-S.; Seo, Y.-T.; Baek, J.; Kim, J.-H.; Park, J.; Kim, S.; Kim, Y.-K.; Hyeon, T.; Cho, M.-H. *Small* **2010**, *6*, 119–125.
(3) Vo-Dinh, T.; Wang, H.-W.; Scaffidi, J. *J. Biophotonics* **2010**, *3*, 89–102.
(4) Hering, K.; Cialla, D.; Ackermann, K.; Doerfer, T.; Moeller, R.; Schneidewind, H.; Mattheis, R.; Fritzsche, W.; Roesch, P.; Popp, J. *Anal. Bioanal. Chem.* **2008**, *390*, 113–124.
(5) Porter, M. D.; Lipert, R. J.; Siperko, L. M.; Wang, G.; Narayanan, R. *Chem. Soc. Rev.* **2008**, *37*, 1001–1011.
(6) Han, X. X.; Zhao, B.; Ozaki, Y. *Anal. Bioanal. Chem.* **2009**, *394*, 1719–1727.
(7) Kneipp, K.; Kneipp, H.; Bohr, H. G. Single-Molecule SERS Spectroscopy. In *Surfaced-Enhanced Raman Scattering—Physics and Applications*; Springer-Verlag: Berlin, Germany, 2006; Vol. 103.
(8) Braun, G.; Lee, S. J.; Dante, M.; Nguyen, T.-Q.; Moskovits, M.; Reich, N. *J. Am. Chem. Soc.* **2007**, *129*, 6378–6379.
(9) Fabris, L.; Dante, M.; Braun, G.; Lee, S. J.; Reich, N. O.; Moskovits, M.; Nguyen, T.-Q.; Bazan, G. C. *J. Am. Chem. Soc.* **2007**, *129*, 6086–6087.

10.1021/ac1023843
Published on Web 12/01/2010

ated target DNA sequences has been successfully demonstrated.[11−13]

Although many SERS-based detection assays are being developed for eventual incorporation into the high-throughput analysis of target analytes, there is nevertheless a need for cost-effective assays that can be performed in the field, or in a point-of-care facility, using portable, operator-friendly Raman spectroscopic instrumentation. NP-based nucleic acid hybridization assays conducted in small solution volumes are particularly suited for this application, as reactions can be performed more rapidly for biological assay reagents having low diffusion coefficients[14] and spectroscopic readings can be rapidly acquired without the need to scan analyte-captured detection films using costly Raman microscopic instrumentation. Despite these advantages, however, NP-based SERS signaling is highly dependent on the formation of aggregates for localized "hot spot" formation, a process that is difficult to experimentally control for reproducible detection sensitivity.[15] In contrast to DNA detection limits in the micromolar range, which have been reported for assays in which target sequence capture is measured using minimally aggregated NP suspensions,[16,17] chemical[18,19] and photoligation-induced[20] aggregate complex formation provides LODs that are in the low-nanomolar range.

In the present study, we describe a paramagnetic NP (MNP) capture SERS assay in which target DNA detection is enhanced in a manner analogous to aggregation by the magnetic pull-down and concentration of hybridization complexes. Au NPs (GNPs) stably conjugated with reporter oligonucleotide probes via a Raman reporter linker are first hybridized with a West Nile virus (WNV) target DNA sequence and MNPs conjugated with capture oligonucleotide probes. Upon the application of an external magnet source, GNP−WNV target sequence−MNP hybridization complexes are immediately removed from solution and the compacted pellet is interrogated with a laser. The LOD for WNV target sequence capture is 10 pM, a 6-fold order of magnitude increase over the sensitivity previously reported for the detection of HIV DNA by Raman microscopy incorporating a magnetic separation step.[21] In summary, this assay format provides a means for rapid analysis owing to the absence of mass transfer limitations during the solution phase hybridization reactions and to the immediate separation and localization of the magnetic pellet within the interrogating laser spot.

EXPERIMENTAL SECTION

Reagents. *N*-Hydroxysuccinimide (NHS)−PEG_2−maleimide ($SM(PEG)_2$) was obtained from Thermo Fisher Scientific, and colloidal GNPs were from Ted Pella Inc. (30 nm, 2×10^{11} NPs/mL). Unless indicated otherwise, all other chemicals and materials were purchased from Sigma-Aldrich. The DNA sequences of the WNV target oligonucleotide (REG2-TARGET53) and the Bluetongue virus (BTV) control target oligonucleotide have been published elsewhere.[17] The sequence and end terminal modification for the reporter probe, REG2-AS2-NH5, is 5′-/5AmMC6/-GTT GGT TTC ACA CTC TTC CGG CTG T-3′, and for the capture probe, REG2-AS1-SH3, it is 5′-ATC ACC CTG CTC GCC TTG AAG TTA GC-/3ThioMC3-D/-3′. All of the oligonucleotides used in these experiments were HPLC-purified and validated by quality control mass spectroscopy (IDT, Inc. Coralville, IA).

Preparation of GNPs Conjugated with Raman Label and Reporter Oligonucleotides. The synthesis of the Raman reporter label 5,5′-dithiobis(succinimidy-2-nitrobenzoate) (DSNB) and its subsequent attachment to 6 mL of colloidal GNPs was conducted according to Grubisha et al.[22] To attach the amino-terminal reporter probe, REG2-AS2-NH5, to the succinimidyl group of DSNB, DSNB-conjugated GNPs and 3.5 μM reporter probe in phosphate-buffered saline (PBS; 10 mM NaPO4, 300 mM NaCl) pH 7.4 were incubated overnight at room temperature. Excess unconjugated reporter probe was subsequently removed by centrifugation (10 000*g* for 7 min.), and the GNP−DSNB−reporter probe pellet was washed and resuspended in 3 mL of PBS pH 7.4 for use in DNA hybridization reactions.

Preparation of Silica Shell-Coated MNPs Conjugated with Capture Oligonucleotides. MNPs were prepared according to Lee et al.[23] Briefly, 1.75 g of sodium dodecylbenzenesulfonate was sonicated in 15 mL of xylene and then mixed with 0.75 mL of 0.75 mM $FeCl_2$ and 1.5 mM $Fe(NO_3)_3$ in water. Following overnight incubation at room temperature, the reverse-micelle suspension was heated to 90 °C and 1 mL of hydrazine was added for the formation of MNPs. To coat the MNPs with amine-functionalized SiO_2, the MNPs were cooled to 40 °C and mixed with 2 mL of a 1:1 solution of tetraethyl orthosilicate (TEOS) and (3-aminopropyl) triethoxysilane (APTES). The final sample was washed with ethanol, precipitated by magnetic pull-down, and then washed several times with PBS pH 8.0 and adjusted to a concentration of 0.73 mg/mL MNPs in PBS pH 8.0.

The *N*-hydroxysuccinimide- and maleimide-activated pegylated linker, $SM(PEG)_2$, was added to 5 mL of the silica-coated MNPs at a final concentration of 5 mg/mL. After an 8 h incubation at room temperature, amide-linked $SM(PEG)_2$−MNP conjugates were separated from solution by magnetic capture and washed several times with PBS pH 7.0 to remove unreacted linker. To generate MNP−$SM(PEG)_2$−oligonucleotide probe conjugates, thiol-modified REG2-AS1-SH3 capture probe was added to MNP−linker conjugates at a final concentration of 3.5 μM and the mixture was then incubated overnight at room temperature.

(10) Fang, C.; Agarwal, A.; Duddharaju, K. D.; Khalid, N. Z.; Salim, S. M.; Widjaja, E.; Garlan, M. V.; Balasubramanian, N.; Kwong, D.-L. *Biosens. Bioelectron.* **2008**, *24*, 216–221.
(11) Cao, Y.-W. C.; Jin, R.; Mirkin, C. A. *Science* **2002**, *297*, 1536–1540.
(12) Sun, L.; Yu, C.; Irudayaraj, J. *Anal. Chem.* **2008**, *80*, 3342–3349.
(13) Kang, T.; Yoo, S. M.; Yoon, I.; Lee, S. Y.; Kim, B. *Nano Lett.* **2010**, *10*, 1189–1193.
(14) Sheehan, P. E.; Whitman, L. J. *Nano Lett.* **2005**, *5*, 803–807.
(15) Sanchez-Cortes, S.; Garcia-Ramos, J. V.; Morcillo, G.; Tinti, A. *J. Colloid Interface Sci.* **1995**, *175*, 358–368.
(16) Wabuyele, M. B.; Vo-Dinh, T. *Anal. Chem.* **2005**, *77*, 7810–7815.
(17) Harpster, M. H.; Zhang, H.; Sankara-Warrier, A. K.; Ray, B. H.; Ward, T. R.; Kollmar, J. P.; Carron, K. T.; Mecham, J. O.; Corcoran, R. C.; Wilson, W. C.; Johnson, P. A. *Biosens. Bioelectron.* **2009**, *25*, 674–681.
(18) Graham, D.; Thompson, D. G.; Smith, W. E.; Faulds, K. *Nat. Nanotechnol.* **2008**, *3*, 548–551.
(19) Qian, X.; Zhou, X.; Nie, S. *J. Am. Chem. Soc.* **2008**, *130*, 14934–14935.
(20) Thuy, N. T. B.; Yokogawa, R.; Yoshimura, Y.; Fujomoto, K.; Koyano, M.; Maenosono, S. *Analyst* **2010**, *135*, 595–602.
(21) Liang, Y.; Gong, J. L.; Huang, Y.; Zheng, Y.; Jiang, J.-H.; Shen, G.-L.; Yu, R.-Q. *Talanta* **2007**, *72*, 443–449.
(22) Grubisha, D.; Lipert, R. J.; Park, H.-Y.; Driskell, J.; Porter, M. D. *Anal. Chem.* **2003**, *75*, 5936–5943.
(23) Lee, J.; Lee, Y.; Youn, J. K.; Na, H. B.; Yu, T.; Kim, H.; Lee, S.-M.; Koo, Y.-M.; Kwak, J. H.; Park, H. G.; Chang, H. N.; Hwang, M.; Park, J.-G.; Kim, J.; Hyeon, T. *Small* **2008**, *1*, 143–152.

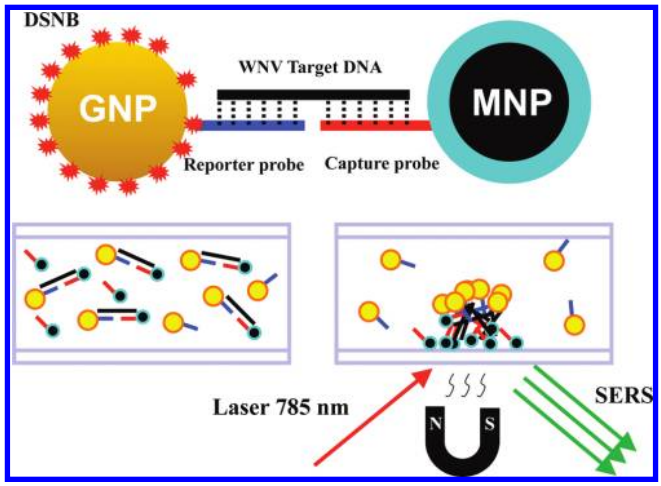

Figure 1. SERS detection of MNP-captured hybridization complex containing WNV target DNA sequence.

Following magnetic capture, the capture probe-conjugated MNPs were washed repeatedly and resuspended in 5 mL of PBS pH 7.4 for use in target sequence detection experiments.

Characterization of Fabricated Capture MNPs and Reporter GNPs. Proton NMR analysis of synthesized DSNB was conducted using a Bruker model ARX-400 spectrometer (Billerica, MA). Transmission electron microscopy (TEM) imaging of NPs deposited on formaver-coated, mesh copper grid films (Electron Microscopy Sciences, Hatfield, PA) was performed using a Hitachi-H7000 TEM (Hitachi Hi-Tech, Tokyo). NP samples for TEM analysis were prepared by briefly dipping the grid films in very dilute solutions to prevent further aggregation during drying. NP size distributions were determined by Dynamic Light Scattering (DLS) using a ZetaPALS spectrometer (Brookhaven Instruments, Holtsville, NY). X-ray photoelectron spectroscopy (XPS) spectra of dried samples of MNP and GNP assemblies on glass slides were acquired at room temperature using the PE 5800 multitechnique surface analysis system (Physical Electronics, Eden Prairie, MN). The system is equipped with a hemispherical analyzer, a multichannel detector at 45°, and monochromatic Al KR excitation radiation (1486.6 eV, 350 W). A pass energy of 23.35 eV was used, giving a half-width of the Au ($4f_{7/2}$) peak of ~0.8 eV. The Au 4f energies were adjust to 83.8 eV for purposes of reporting peak position. XPS traces were deconvoluted into separate peaks using the software program XPS Peak 4.1.

SERS Detection of WNV Target DNA by Magnetic Capture. DNA hybridization reactions were conducted using 1 mL of reporter probe-conjugated GNPs, 0.5 mL of capture-probe conjugated MNPs, and target and control DNA sequences in PBS pH 7.4. All hybridization reactions were conducted in capped glass vials for 1 h at room temperature, after which the hybridization complexes were precipitated from solution using a small external magnet. Laser excitation of concentrated sample pellets was performed using an Advantage NIR Raman spectrometer (DeltaNu Inc., Laramie, WY) (60 mW power, 785 nm laser) fitted with right-angle input optics. The scheme summarizing WNV DNA capture and detection is illustrated in Figure 1, and the chemical structures of fabricated reporter GNPs and capture MNPs are shown in Figure 2. Spectral data was acquired using NuSpec software and recorded in the 200−2000 vibrational unit range (Raman shift/cm^{-1}), with the baseline off, the resolution set a low, and an integration

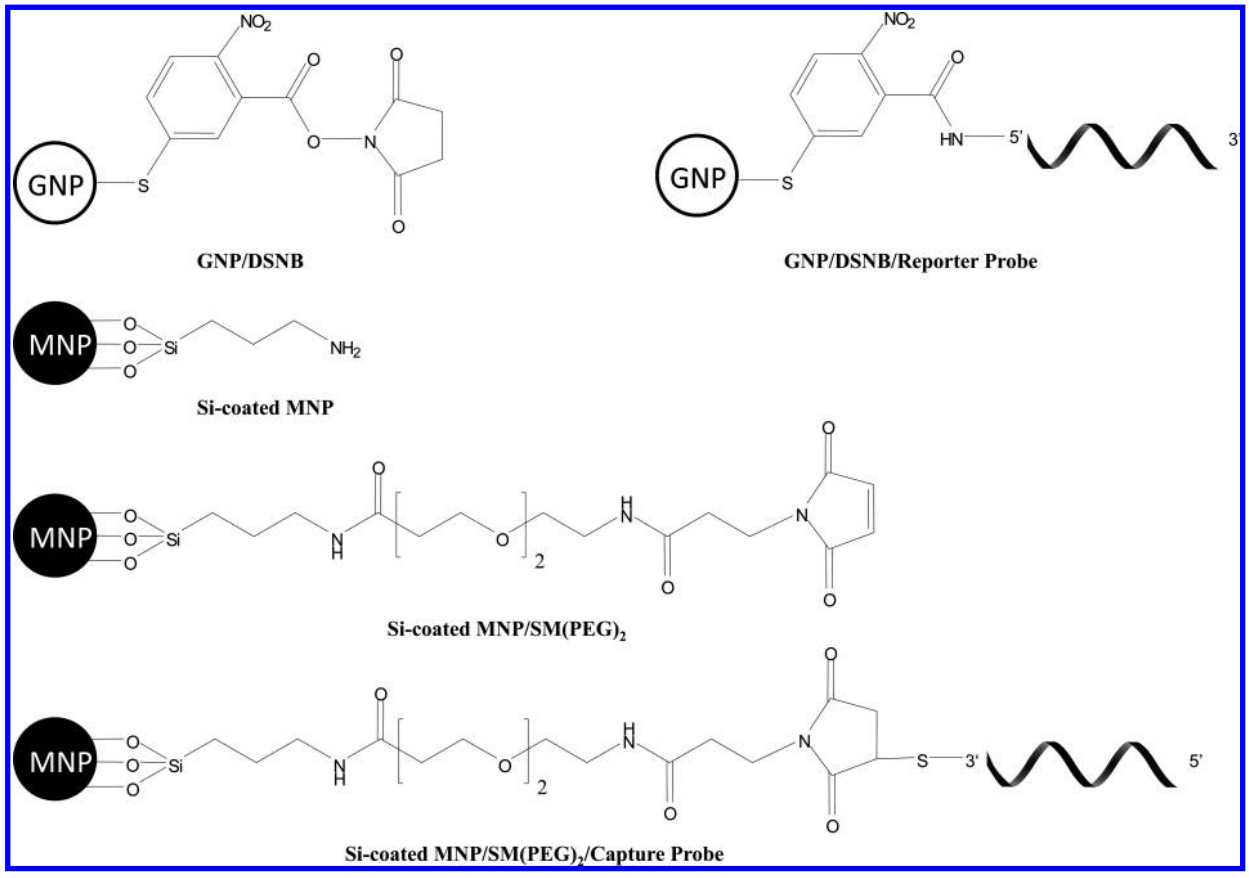

Figure 2. Chemical structures of reporter GNPs and capture MNPs at successive steps in the fabrication process.

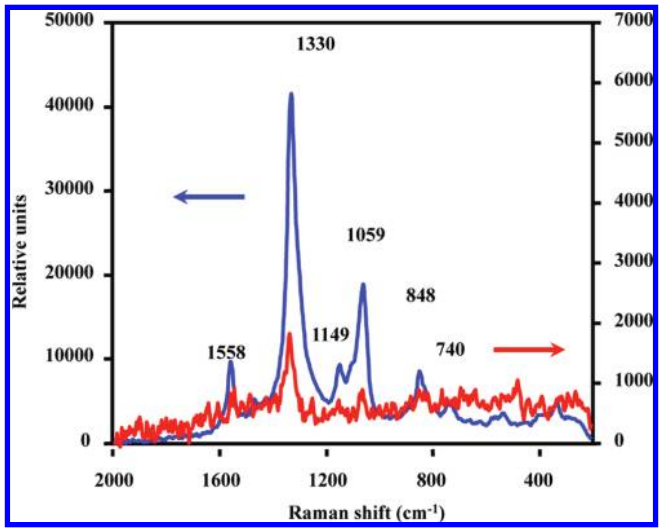

Figure 3. SERS spectra for DNA-functionalized DSNB-coated GNPs in 600 μL of water (red spectrum, 2×10^{11} NPs/mL) and 20 μL of the same sample air-dried on a glass slide (blue spectrum).

time of 5 s. Grams/AI software (Thermo Fisher Scientific) was employed for data interpretation and manipulation.

RESULTS AND DISCUSSION

Fabrication of Reporter GNPs and Capture MNPs. The structure of the Raman label used in these studies, DSNB, was validated by ^{1}H NMR following its synthesis and recrystallization from hexane/acetone according to Grubisha et al.[22] (Supporting Information Figure S-1). Thiolated DSNB conjugates of GNPs in aqueous solution and dried onto glass slides were analyzed by Raman spectroscopy (data not shown). As the final step in the preparation of reporter GNPs, the amino-modified reporter oligonucleotide, REG1-AS2-NH5, was stably conjugated to DSNB-coated GNPs via amide linkage with the succinimide ester group of DSNB. As shown in Figure 3, laser excitation of dried DNA-functionalized DSNB-coated GNP samples provided discrete vibrational peaks at 1558, 1330, 1149, 1059, 848, and 740 cm^{-1} that align with SERS spectra previously reported for DSNB.[22,24] Aqueous samples, however, provided weakly intensified spectra in which the dominant 1330 and 1059 cm^{-1} peaks were reduced by nearly 20-fold in signal peak height. These results demonstrate GNP coverage with DSNB and the dependence of DSNB detection sensitivity on sequestration within the localized enhanced electromagnetic fields of concentrated NP SERS substrates.[25]

Silica coated MNPs functionalized with amine groups were imaged by TEM to determine the extent of particle dispersion versus aggregation. Although discrete nanoparticles of ~6−7 nm in size were observed (Supporting Information Figure S-2), the bulk of MNP preparations consisted of aggregated complexes of >200 nm in average size corroborated by dynamic light scattering (DLS) and TEM (see Table 2, Supporting Information Figure S-3, and Figure 6). Aggregation is commonly observed for amine-functionalized silica-coated MNPs[21,26] and, according to Bagwe et al.,[27] is attributed to nonspecific interparticle binding interactions arising from the hydrolytic polycondensation of TEOS and APTES and the absence of further silica surface modification with inert functional groups. To develop stable thioether bioconjugates of the thiol-modified capture oligonucleotide, REG1-AS1-SH3, with amine-functionalized MNPs, we used SM(PEG)$_2$ as a surface tethering linker.

Table 1. XPS Binding Energies (eV) for GNP and MNP Assemblies

Atomic composition	GNP/DSNB	GNP/DSNB/ Reporter probe
Au (4f7/2)	83.8	83.8
S (2p3/2)	161.9	161.8
S (2p1/2)	163.1	163
C (1s)	284.7, 286.3, 288.3	284.7, 286.0, 288.5
N (1s)	405.4, 401.1	405.4, 401.3, 399.6
O (1s)	532.1, 534.0	532.4,534.4
P (2p)	nd	134.1

Atomic composition	Si-coated MNP	Si-coated MNP/SM(PEG)$_2$	Si-coated MNP/ SM(PEG)$_2$/ Capture probe
Fe (2p3/2)	712.1	711.7	nd
Fe (2p1/2)	724.8	724.7	nd
Si (2p)	102.4−103.7	102.4−103.7	102.4−103.7
O (1s)	533.6, 531.7	533.5, 532.6, 531.2	533.6, 532.9
C (1s)	285.8, 287.0	285.7, 286.9, 287.5, 289.4	285.9, 287.0, 287.7, 289.1
N (1s)	400.6, 402.1	400.6, 402.0	400.9, 402.9
P (2p)	nd	nd	134.2
S (2s)	nd	nd	227.2

XPS Characterization of Reporter GNPs and Capture MNPs. XPS analysis of NP assemblies was undertaken to determine element and chemical bond compositions and thereby confirm GNP and MNP surface modifications. In agreement with the structure of DSNB (Figure 2), wide-scan XPS survey spectra for DSNB-conjugated GNPs provided binding energy peaks that indicate the presence of Au, S, C, O, and N (Table 1). Peak values recorded for the Au ($4f_{7/2}$), C (1s), S ($2p_{3/2}$), and S ($2p_{1/2}$) electron orbital regions are in accordance with the binding energies measured for these regions in a study which reported on the assembly of functionalized benzophenone derivatives on Au films.[28] The S ($2p_{3/2}$) and S ($2p_{1/2}$) doublet at 161.9 and 163.1 eV is consistent with the presence of Au-bound thiolates, and the C (1s) 288.3, 286.3, and 284.7 eV peaks correspond to carbonyl C's, the lower energy C−O, C−N, and C−S bonds, and alkyl C's, respectively. For the O (1s) region, the O of the aromatic nitro group is indicated by the peak at 532.1 eV[29] and the peak at 534 eV is characteristic of carbonyl O's in the presence of metals.[30] The change in the spectrum for the N (1s) region following conjugation with the reporter probe is diagnostic for the presence of DNA. GNP/DSNB a is characterized by two peaks: a higher energy peak at 405.4 eV which

(24) Ryu, K.; Haes, A. J.; Park, H.-Y.; Nah, S.; Kim, J.; Chung, H.; Yoon, M.-Y.; Han, S.-H. *J. Raman Spectrosc.* **2010**, *41*, 121–124.
(25) Kovacs, G. J.; Loutfy, R. O.; Vincett, P. S. *Langmuir* **1986**, *2*, 689–694.
(26) Gong, J. L.; Liang, Y.; Chen, J.-W.; Jiang, J.-H.; Shen, G.-L.; Yu, R.-Q. *Biosens. Bioelectron.* **2007**, *22*, 1501–1507.
(27) Bagwe, R.; Hilliard, L. R.; Tan, W. *Langmuir* **2006**, *22*, 4357–4362.
(28) Delamarche, E.; Sundarababu, G.; Biebuyck, H.; Michel, B.; Gerber, C.; Sigrist, H.; Wolf, H.; Ringsdorf, H.; Xanthopoulos, N.; Mathieu, H. J. *Langmuir* **1996**, *12*, 1997–2006.
(29) Zaugg, F. G.; Spencer, N. D.; Wagner, P.; Kernen, P.; Vinckier, A.; Groscurth, P.; Semsenza, G. *J. Mater. Sci.: Mater. Med.* **1999**, *10*, 255–263.
(30) Sharma, J.; Owens, F. J. *Chem. Phys. Lett.* **1979**, *61*, 280–283.

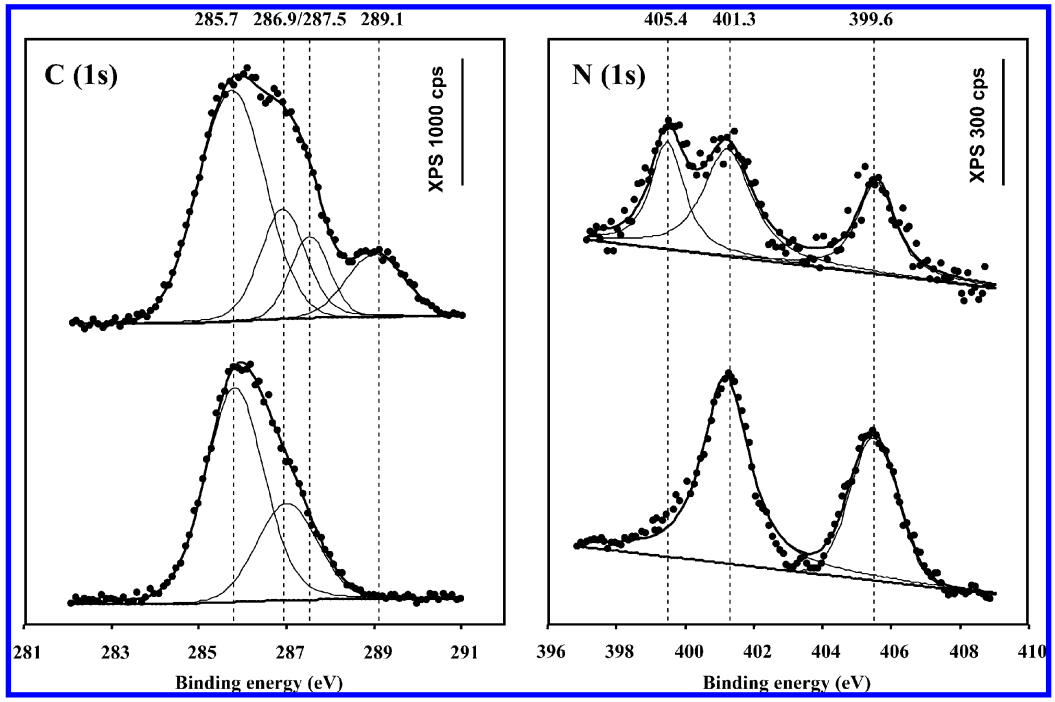

Figure 4. XPS C (1s) spectra for silica-coated MNPs (bottom spectrum) and silica-coated MNPs fabricated with $SM(PEG)_2$ (top spectrum) and XPS N (1s) spectra for DSNB-conjugated GNPs (bottom spectrum) and DSNB-conjugated GNPs fabricated with reporter probe (top spectrum). The filled circles indicate raw data measurements, and the solid lines define fitted peaks that were calculated from deconvoluted raw data. cps = counts/s.

is attributed to the nitro functional group[31] and a lower energy peak at 401.1 eV corresponding to the succinimidyl N[32] (Table 1). Following amide linkage of the reporter oligonucleotide, we detected a negligible shift in the 401.1 eV peak, which reflects the removal of succinimidyl N,[33] and the appearance of a distinct peak at 399.6 eV, which is ascribed to heterocyclic N atoms[34,35] (Figure 4). The single peak at 134.1 eV in the P (2p) region supports this interpretation and is diagnostic for the phosphoester bonds of the DNA backbone[36] (Table 1 and Supporting Information Figure S-3).

The XPS spectra for silica-coated MNPs exhibited peaks in the 102.4−103.7 eV range corresponding to the Si (2p) region, and two distinct peaks for Fe that correspond to the $2p_{3/2}$ and $2p_{1/2}$ orbitals of iron oxides were undetectable following conjugation with the capture oligonucleotide (Table 1). Although we have recorded Fe peaks for silica-coated MNPs modified with the $SM(PEG)_2$ linker, Kang et al.[37] have observed that binding energy peaks associated with Fe in unmodified magnetic cores particles are absent following silica coating. Additional XPS spectra which support the successful coating of magnetic core particles with silica and their subsequent conjugation with $SM(PEG)_2$ are indicated by the 533.5−533.6 eV peak (Si−O bond) and 532.6 eV carbonyl bond peak of O (1s)[38] and N (1s) peaks denoting the secondary and tertiary amines (400.6 and 400.9 eV).[39] Highlighted C bond interactions of $SM(PEG)_2$-coated MNPs are indicated by the low-energy alkyl C peak (285.7 eV), higher energy C bonds (i.e., C−N and C−Si) (286.7 eV), C−O−C ether bonds (287.5 eV), and carbonyl Cs (289.4 eV) of the C (1s) region[28,40,41] (Figure 4). Spectra supporting thioether linkage of the capture oligonucleotide are demonstrated by the 227.2 eV peak for the S (2s) region[42] and the 134 eV P (2p) peak for phosphoester bonds (Supporting Information Figure S-3).

DLS Measurements of Fabricated Reporter GNPs and Capture MNPs. To characterize the physical properties of NP assemblies further, DLS measurements were conducted at each step of the fabrication process. As shown in Table 2, the incremental increase in the average diameter of GNPs associated with the layering of DSNB and reporter oligonucleotide probe is consistent with the small molecular structure of DSNB and the compact structures observed for single-stranded (ss) oligonucleotides on Au surfaces.[43] On the basis of the approximate base-to-base distance of 0.7 nm for ss DNA,[44] we would predict an

(31) Bjorneholm, O.; Nilsson, A.; Zdansky, O. F.; Sandell, A.; Hernnas, B.; Tillborg, H. *Phys. Rev. B* **1992**, *46*, 1053–10365.
(32) Wei, J.; Hing, P.; Mo, Z. Q. *Surf. Interface Anal.* **1999**, *28*, 208–211.
(33) Xiao, S.-J.; Brunner, S.; Wieland, M. *J. Phys. Chem. B* **2004**, *108*, 16508–16517.
(34) Johnson, P. A.; Levicky, R. *Langmuir* **2003**, *19*, 10288–10294.
(35) Lee, C.-H.; Gong, P.; Harbers, G. M.; Grainger, D. W.; Castner, D. G.; Gamble, L. J. *Anal. Chem.* **2006**, *78*, 3316–3325.
(36) Kulkarni, S. K.; Ethiraj, A. S.; Kharrazi, S.; Deobagkar, D. N.; Deobagkar, D. D. *Biosens. Bioelectron.* **2005**, *21*, 95–102.
(37) Kang, K.; Choi, J.; Nam, J. H.; Lee, S. C.; Kim, K. J.; Lee, S.-W.; Chang, J. H. *J. Phys. Chem. B* **2009**, *113*, 536–543.
(38) Barr, T. L. *Zeolites* **1990**, *10*, 760–765.
(39) Kim, T. H.; Choi, H. S.; Go, B. R.; Kim, J. *Electrochem. Commun.* **2010**, *12*, 788–791.
(40) Sharma, S.; Johnson, R. W.; Desai, T. A. *Biosens. Bioelectron.* **2004**, *20*, 227–239.
(41) Wallart, X.; de Villeneuve, C. H.; Allongue, P. *J. Am. Chem. Soc.* **2005**, *127*, 7871–7878.
(42) Becker, U.; Hochella, M. F., Jr. *Geochim. Cosmochim. Acta* **1996**, *60*, 2413–2426.
(43) Levicky, R.; Herne, T. M.; Tarlov, M. J.; Satija, S. K. *J. Am. Chem. Soc.* **1998**, *120*, 9787–9792.
(44) Grange, W.; Duckely, M.; Husale, S.; Jacob, S.; Engel, A.; Hegner, M. *PLoS Biol.* **2008**, *6*, 0343–0351.

Table 2. DLS Measurements of GNP and MNP

GNP	GNP/DSNB	GNP/DSNB/ Reporter Probe
31.1 ± 6.7 nm	35.2 ± 6.5 nm	47.2 ± 18 nm
Si-coated MNP	Si-coated MNP/ $SM(PEG)_2$	Si-coated MNP/ $SM(PEG)_2$/capture probe
202 ± 81 nm	249.1 ± 104 nm	251 ± 110 nm

average particle diameter of ~70 nm for fully extended oligonucleotides having a length of 25 bases. In contrast to GNP assembly, DLS measurements of the successive layering of $SM(PEG)_2$ and capture oligonucleotide probe on amine-functionalized silica-coated MNPs are less informative. Due to the high margin of error recorded for the radii of aggregated MNPs, it is difficult to unambiguously ascribe changes in the hydrodynamic radii of particle clusters with the formation of multilayered surface assemblies.

SERS Detection of Magnetically Captured WNV Target Sequence. SERS spectra for WNV target sequence detection were acquired by first hybridizing reporter probe-conjugated GNPs and capture probe-conjugated MNPs with WNV target oligonucleotide and then concentrating hybridization complexes by an external magnet source for subsequent laser interrogation. Negative control hybridization reactions consisted of the absence of target sequence and the substitution of a 50 base nonspecific oligonucleotide derived from the BTV genome. All hybridization reactions were conducted in 1.5 mL of high-salt (i.e., 0.32 M $[Na^+]$) buffer and contained ~2.7×10^{11} reporter GNPs/mL and ~0.24 mg/mL of capture MNPs. Although we do not have quantitative measurements for dispersed and aggregate NP probe coverage, we assume that either the capture or reporter probe is limiting for GNP−WNV target−MNP complex formation and have ensured that probe concentrations are in sequence excess relative to the range of input target sequence concentrations tested in these experiments.

As shown in Figure 5A, SERS detection of WNV target sequence at a concentration of 100 nM is indicated by an intense spectral peak profile specific for DSNB (Figure 5A, spectrum a). Hybridizations containing the BTV control sequence, however, reveal only trace amounts of the dominant 1330 cm^{-1} peak (Figure 5A, spectrum b), the area of which is reduced by more than 200-fold relative to the same peak in spectrum a in Figure 5A. Negative control spectra for hybridization reactions containing only reporter GNPs and capture MNPs are similar to the spectrum for BTV (Figure 5A, spectrum c), indicating that the weak SERS signaling recorded for these controls is due to the low-level, nonspecific interaction of fabricated GNPs and MNPs. Of particular note, we have found that the SERS spectra for WNV target sequence hybridizations that have not been concentrated by magnetic pull-down provide spectra similar to the negative control hybridizations (Figure 5A, spectrum d). This demonstrates the dependence of robust SERS signaling on magnetic concentration within the laser spot and further suggests that the hybridization-dependent localization of DSNB on the highly irregular surfaces of dispersed MNP aggregates is insufficient for facilitating levels of detection above background. To determine the LOD sensitivity for WNV target sequence detection, SERS spectra were acquired for DNA hybridizations containing dilutions of the WNV oligonucleotide. Figure 5B shows that there is a progressive decrease in SERS signaling as the concentration of target sequence is reduced from 100 nM to 10 pM. The spectra were background-corrected, and the averages of the height of the 1330 cm^{-1} peaks were plotted versus target DNA concentration (pM) in Figure 5C. Linear regression analysis of the peak height versus $\log_{10}$ of the target DNA concentration yields an R^2 value of 0.93.

Additional evidence supporting the dependence of the physical interaction of reporter GNPs and capture MNPs on SERS signaling is shown in TEM images of hybridization reaction samples. Hybridizations conducted in the presence of WNV oligonucleotide (Figure 6, upper panel) clearly illustrate the binding of high contrast GNPs with the outer surfaces of aggregated MNPs. When the target sequence is omitted from the hybridization reaction,

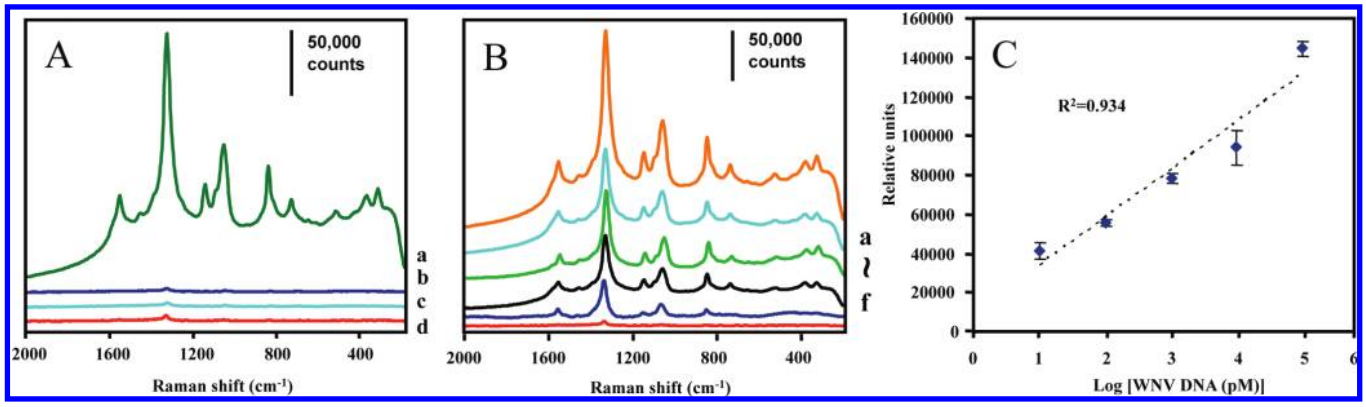

Figure 5. SERS spectra for WNV target sequence capture. (A) Stacked spectra for magnetically pulled-down DNA hybridization containing reporter GNPs, capture MNPs, and WNV target DNA (spectrum a), magnetically pulled-down reporter GNP, capture MNP, and BTV target hybridization (spectrum b), magnetically pulled-down hybridization reaction containing only reporter GNPs and capture MNPs (spectrum c), and reporter GNPs, capture MNPs, and WNV target DNA hybridization in solution (spectrum d). (B) Stacked spectra for DNA hybridizations containing dilutions of WNV target DNA: 100 nM (spectrum a), 10 nM (spectrum b), 1 nM (spectrum c), 100 pM (spectrum d), 10 pM (spectrum e). The spectra shown here are representative of three independent repetitions for each of the experimental conditions listed. cts/s = counts/s. (C) Plot of SERS intensity at peak 1330 cm^{-1} vs $\log_{10}$ concentration target sequence DNA. Data points represent averages of three independent sample measurements, and error bars denote one standard deviation from the mean.

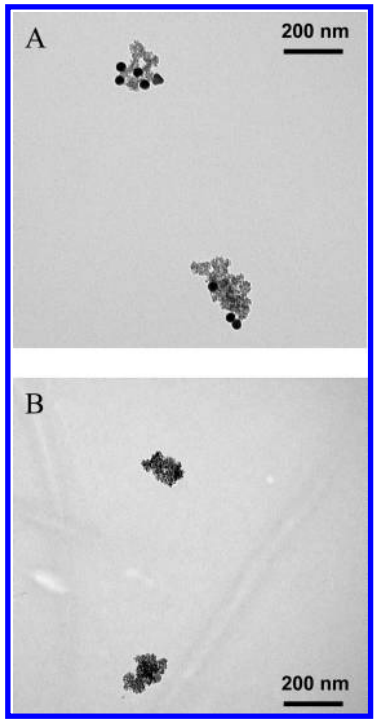

Figure 6. TEM images of DNA hybridization reactions conducted in the presence (upper panel) and absence (lower panel) of WNV target sequence. Aliquots were removed from reactions that had gone to completion and briefly centrifuged. Pelleted hybridization complexes were then washed with PBS pH 7.4 to remove unhybridized reporter GNPs and then sonicated for 1 min in the same buffer prior to TEM analysis.

however, we have been unable to obtain images that could be interpreted as demonstrating the physical association of GNPs with MNPs (Figure 6, lower panel).

CONCLUSION

In the work presented here, we have demonstrated a NP-based, proof-of-concept SERS assay for the sensitive detection of magnetically captured DNA derived from the WNV RNA genome. The assay is rapid and requires approximately 1 h to perform from the time of assembling fabricated reporter GNPs and capture MNPs with the target oligonucleotide analyte to acquiring SERS spectra for the laser excitation of hybridization complexes that have been pulled out of solution and concentrated by magnetic pull-down. As spectra are easily acquired at the benchtop by simply directing the laser beam at pelleted material collected in small glass vials, the assay affords the opportunity of integration within a portable Raman spectroscopic detection format which is engineered for accommodating DNA hybridization and target sequence detection within a single vial. Before efforts in this endeavor can be initiated, however, it will be necessary to identify critical features of the current assay that can be optimized for enhancing detection sensitivity, thereby establishing LODs that are relevant in a diagnostic setting. Currently, magnetic capture-based SERS immunoassays have reported LODs for the tumor marker, human α-fetoprotein,[26] and a lung cancer marker, carcinoembryonic antigen,[45] which are considerably lower than the LODs that have been reported for DNA detection. Although nucleic acid capture necessarily presents a number of technical challenges that are not encountered in the detection of antigen−antibody interactions, it is nevertheless a goal in the development of SERS-based nucleic acid detection assays to develop simplified, cost-effective assay platforms that do not require target amplification and which also compete with, or even surpass, qRT-PCR technologies in analyte detection sensitivity.

ACKNOWLEDGMENT

We gratefully acknowledge the assistance and technical expertise of Dr. Patrick McCurdy (Surface Analysis Laboratory, Colorado State University, Ft. Collins, CO) in performing XPS analysis. Support in the early stages of this work was provided by financial support from the Rocky Mountain Regional Center for Excellence (NIH Grant AI-065357-03). The contents of this publication are the responsibility of the authors and do not necessarily represent the views of NIH or the USDA.

SUPPORTING INFORMATION AVAILABLE

Figures S-1, S-2, S-3, and S-4. This material is available free of charge via the Internet at http://pubs.acs.org.

Received for review September 7, 2010. Accepted November 4, 2010.

AC1023843

(45) Chon, H.; Lee, S.; Son, S. W.; Oh, C. H.; Choo, J. *Anal. Chem.* **2009**, *81*, 3029–3034.